

# FERMI NATIONAL ACCELERATOR LABORATORY

FERMILAB-CONF-16-295-E

TEVEWWG/WZ2016/01

CDF Note 11203

D0 Note 6487

31 July 2016

## Combination of the CDF and D0 effective leptonic electroweak mixing angles

The Tevatron Electroweak Working Group<sup>1</sup>

for the CDF and D0 Collaborations

CDF and D0 have measured the effective leptonic weak mixing angle  $\sin^2 \theta_{\text{eff}}^{\text{lept}}$ , using their full Tevatron datasets. This note describes the Tevatron combination of these measurements, and the ZFITTER standard model-based inference of the on-shell electroweak mixing angle  $\sin^2 \theta_W$ , or equivalently, the  $W$ -boson mass. The combination of CDF and D0 results yields:

$$\sin^2 \theta_{\text{eff}}^{\text{lept}} = 0.23179 \pm 0.00035, \text{ and}$$

$$\sin^2 \theta_W = 0.22356 \pm 0.00035, \text{ or equivalently,}$$

$$M_W(\text{indirect}) = 80.351 \pm 0.018 \text{ GeV}/c^2.$$

---

<sup>1</sup> The Tevatron Electroweak Working Group can be contacted at [tev-ewwg@fnal.gov](mailto:tev-ewwg@fnal.gov).  
More information can be found at <http://tevewwg.fnal.gov>.

## I. INTRODUCTION

At the Fermilab Tevatron proton-antiproton ( $p\bar{p}$ ) collider, Drell-Yan [1] lepton pairs are produced in the process  $p\bar{p} \rightarrow \ell^+\ell^- + X$  through an intermediate  $\gamma^*/Z$  boson. The forward-backward asymmetry in the polar-angle distribution of the  $\ell^-$  as a function of the  $\ell^+\ell^-$ -pair mass is used to obtain  $\sin^2 \theta_{\text{eff}}^{\text{lept}}$ , the effective leptonic electroweak-mixing parameter  $\sin^2 \theta_W$  [2].

The measured forward-backward asymmetry is compared with templates of the asymmetry calculated with different values of the electroweak mixing parameter to obtain the best-fit value.

### A. Electroweak couplings

The production of Drell-Yan lepton pairs at the Born level proceeds through two parton-level processes,

$$\begin{aligned} q\bar{q} &\rightarrow \gamma^* \rightarrow \ell^+\ell^- \text{ and} \\ q\bar{q} &\rightarrow Z \rightarrow \ell^+\ell^-, \end{aligned} \tag{1}$$

where the  $q$  and  $\bar{q}$  are the quark and antiquark, respectively, from the colliding hadrons. The virtual photon couples the vector currents of the incoming and outgoing fermions ( $f$ ), and the spacetime structure of a photon-fermion interaction vertex is  $\langle \bar{f} | Q_f \gamma_\mu | f \rangle$ , where  $Q_f$ , the strength of the coupling, is the fermion charge (in units of  $e$ ), and  $|f\rangle$  is the spinor for fermion  $f$ . An interaction vertex of a fermion with a  $Z$  boson contains both vector ( $V$ ) and axial-vector ( $A$ ) current components, and its structure is  $\langle \bar{f} | g_V^f \gamma_\mu + g_A^f \gamma_\mu \gamma_5 | f \rangle$ . The Born-level coupling strengths are

$$\begin{aligned} g_V^f &= T_3^f - 2Q_f \sin^2 \theta_W \text{ and} \\ g_A^f &= T_3^f, \end{aligned} \tag{2}$$

where  $T_3^f$  is the third component of the fermion weak-isospin, which is  $T_3^f = \frac{1}{2} (-\frac{1}{2})$  for positively (negatively) charged fermions. At the Born level in the standard model, and in all orders of the on-shell renormalization scheme [3], the  $\sin^2 \theta_W$  parameter is related to the  $W$ -boson mass  $M_W$  and the  $Z$ -boson mass  $M_Z$  by the relationship  $\sin^2 \theta_W = 1 - M_W^2/M_Z^2$ . Since the  $Z$ -boson mass is accurately known (to  $\pm 0.0021 \text{ GeV}/c^2$  [4, 5]), the inference of the on-shell  $\sin^2 \theta_W$  is equivalent to an indirect  $W$ -boson mass measurement.

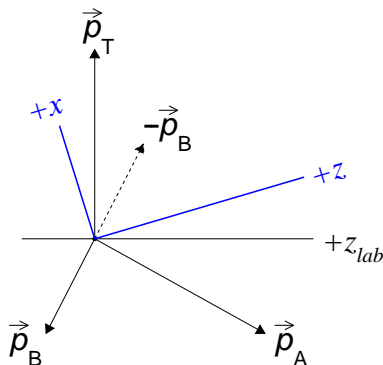


Figure 1: Representation of the Collins-Soper coordinate axes  $(x, z)$  in the lepton-pair rest frame, relative to the laboratory  $z$  axis ( $z_{lab}$ ). These three axes are in the plane formed by the proton ( $\vec{p}_A$ ) and antiproton ( $\vec{p}_B$ ) momentum vectors in the rest frame. The  $z$  axis is the angular bisector of  $\vec{p}_A$  and  $-\vec{p}_B$ . The  $y$  axis is along the direction of  $\vec{p}_B \times \vec{p}_A$ , and the  $x$  axis is in the direction opposite to the transverse component of  $\vec{p}_A + \vec{p}_B$ .

Radiative corrections alter the strength of the Born-level couplings into effective couplings. These effective couplings have been investigated at LEP-1 and SLC [4, 5], at the Tevatron [6–13], and at the LHC [14–16]. The effective  $\sin^2 \theta_W$  coupling at the lepton vertex, denoted as  $\sin^2 \theta_{\text{eff}}^{\text{lept}}$ , has been accurately measured at the LEP-1 and SLC  $e^+e^-$  colliders [4, 5]. The combined average of six individual measurements yields a value of  $0.23149 \pm 0.00016$ . However, there is tension between the two most precise individual measurements: the combined LEP-1 and SLD  $b$ -quark forward-backward asymmetry ( $A_{\text{FB}}^{0,b}$ ) yields  $\sin^2 \theta_{\text{eff}}^{\text{lept}} = 0.23221 \pm 0.00029$ , and the SLD left-right polarization asymmetry of  $Z$ -boson production ( $\mathcal{A}_\ell$ ) yields  $\sin^2 \theta_{\text{eff}}^{\text{lept}} = 0.23098 \pm 0.00026$ . They differ by 3.2 standard deviations.

## B. The forward-backward asymmetry

The angular distribution of leptons from the Drell-Yan process in the rest frame of the boson is governed by the polarization state of the  $\gamma^*/Z$  boson. The polar and azimuthal angles of the  $\ell^-$  direction in the rest frame of the boson are denoted as  $\vartheta$  and  $\varphi$ , respectively. The ideal positive  $z$  axis coincides with the direction of the incoming quark so that the definition of  $\vartheta$  parallels the definition used in  $e^+e^-$  collisions at LEP [4, 5]. This frame is approximated by the Collins-Soper (CS) rest frame [17] for  $p\bar{p}$  collisions, and a view of the frame is shown in Fig. 1.

The CS frame angle,  $\vartheta$  [17], is reconstructed using the following laboratory-frame quantities: the lepton energies, the lepton momenta along the beam line, the dilepton invariant mass,  $M$ , and the dilepton transverse momentum,  $p_T$ . The polar angle of the negatively charged lepton is calculated from

$$\cos \vartheta = \frac{l_+^- l_-^+ - l_-^- l_+^+}{M \sqrt{M^2 + p_T^2}}, \quad (3)$$

where  $l_{\pm} = (E \pm p_z)$  and the  $+$  ( $-$ ) superscript specifies that  $l_{\pm}$  is for the positively (negatively) charged lepton. Similarly, the CS expression for  $\varphi$  in terms of laboratory-frame quantities is given by

$$\tan \varphi = \frac{\sqrt{M^2 + p_T^2}}{M} \frac{\vec{\Delta} \cdot \widehat{R}_T}{\vec{\Delta} \cdot \widehat{p}_T}, \quad (4)$$

where  $\vec{\Delta}$  is the difference between the  $\ell^-$  and  $\ell^+$  lab frame momentum vectors;  $\widehat{R}_T$  is the transverse unit vector along  $\vec{p}_p \times \vec{p}$ , with  $\vec{p}_p$  being the proton momentum vector and  $\vec{p}$  the lepton-pair momentum vector; and  $\widehat{p}_T$  is the unit vector along the transverse component of the lepton-pair momentum vector. At  $p_T = 0$ , the angular distribution is azimuthally symmetric. The right-hand sides of the definitions of  $\cos \vartheta$  and  $\tan \varphi$  are manifestly invariant under Lorentz boosts along the laboratory  $z$  direction.

The general structure of the Drell-Yan lepton angular-distribution in the boson rest frame consists of terms from nine helicity cross-sections that describe the polarization state of the boson,

$$\begin{aligned} \frac{dN}{d\Omega} \propto & (1 + \cos^2 \vartheta) + \\ & A_0 \frac{1}{2} (1 - 3 \cos^2 \vartheta) + \\ & A_1 \sin 2\vartheta \cos \varphi + \\ & A_2 \frac{1}{2} \sin^2 \vartheta \cos 2\varphi + \\ & A_3 \sin \vartheta \cos \varphi + \\ & A_4 \cos \vartheta + \\ & A_5 \sin^2 \vartheta \sin 2\varphi + \\ & A_6 \sin 2\vartheta \sin \varphi + \\ & A_7 \sin \vartheta \sin \varphi, \end{aligned} \quad (5)$$

where each term is relative to the cross section for unpolarized production integrated over the lepton angular distribution [18, 19]. The coefficients  $A_{0-7}$  are functions of kinematic variables

of the boson and vanish when the lepton-pair transverse momentum is zero, except for  $A_4$ , which contributes to the tree-level QCD amplitude and generates the forward-backward  $\ell^-$  asymmetry in  $\cos\vartheta$ . Thus, at zero transverse momentum, the angular distribution reduces to the tree-level form  $1 + \cos^2\vartheta + A_4 \cos\vartheta$ . In the CS frame, the  $A_0$ ,  $A_2$ , and  $A_4$  coefficients are large relative to the other coefficients.

The  $A_4 \cos\vartheta$  term violates parity, and is due to the interference of the amplitudes of the vector and axial-vector currents. Its presence induces an asymmetry in the  $\varphi$ -integrated  $\cos\vartheta$  dependence of the cross section. Two sources contribute: the interference between the  $Z$ -boson vector and axial-vector amplitudes, and the interference between the photon vector and  $Z$ -boson axial-vector amplitudes. The asymmetric component from the  $\gamma^*$ - $Z$  interference cross section contains  $g_A^f$  couplings that are independent of  $\sin^2\theta_W$ . The asymmetric component from  $Z$ -boson self-interference contains a product of  $g_V^\ell$  and  $g_V^q$  from the lepton and quark vertices, and thus is related to  $\sin^2\theta_W$ . At the Born level, this product is

$$T_3^\ell (1 - 4|Q_\ell| \sin^2\theta_W) T_3^q (1 - 4|Q_q| \sin^2\theta_W), \quad (6)$$

where  $\ell$  and  $q$  denote the lepton and quark, respectively. For the Drell-Yan process, the relevant quarks are predominantly the light quarks  $u$ ,  $d$ , or  $s$ . The coupling factor has an enhanced sensitivity to  $\sin^2\theta_W$  at the lepton- $Z$  vertex: for a  $\sin^2\theta_W$  value of 0.223, a 1% variation in  $\sin^2\theta_W$  changes the lepton factor (containing  $Q_\ell$ ) by about 8%, and it changes the quark factor (containing  $Q_q$ ) by about 1.5% (0.4%) for the  $u$  ( $d$  or  $s$ ) quark. Electroweak radiative corrections do not alter significantly this Born-level interpretation. Loop and vertex electroweak radiative corrections give multiplicative form-factor corrections [20–22] to the couplings that change their values by a few percent [7, 8].

The forward-backward asymmetry in  $\cos\vartheta$  is defined as

$$A_{\text{fb}}(M) = \frac{\sigma^+(M) - \sigma^-(M)}{\sigma^+(M) + \sigma^-(M)} = \frac{3}{8} A_4(M), \quad (7)$$

where  $M$  is the lepton-pair invariant mass,  $\sigma^+$  is the total cross section for  $\cos\vartheta \geq 0$ , and  $\sigma^-$  is the total cross section for  $\cos\vartheta < 0$ . Figure 2 shows the typical dependence of the asymmetry as a function of the lepton-pair invariant mass from a Drell-Yan QCD calculation. The offset of  $A_{\text{fb}}$  from zero at  $M = M_Z$  is related to  $\sin^2\theta_W$ . Away from the  $Z$  pole, the asymmetry is dominated by the component from  $\gamma^*$ - $Z$  interference, whose cross section is proportional to  $(M^2 - M_Z^2)/M^2$ , and the asymmetries in these regions are related to the flux of

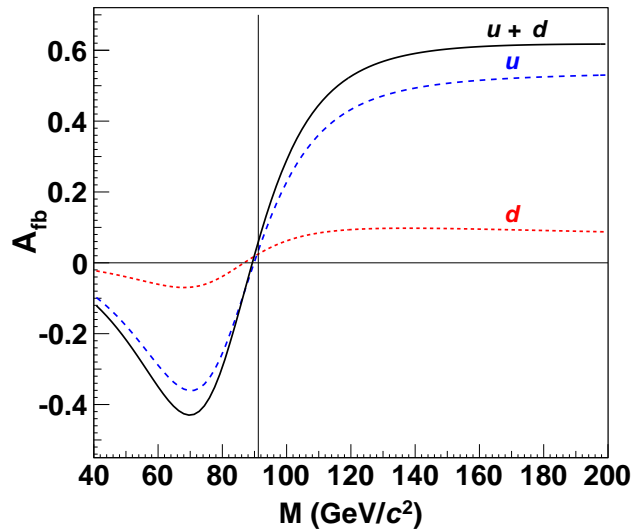


Figure 2: Typical dependence of  $A_{\text{fb}}$  as a function of the lepton-pair invariant mass  $M$ . The vertical line is at  $M = M_Z$ . The label  $u + d$  denotes the overall asymmetry, and the labels  $u$  and  $d$  denote the contribution to the overall asymmetry from quarks with charge  $2/3$  and  $-1/3$ , respectively. The asymmetry identified by the  $u$  or  $d$  label is defined as  $(\sigma_q^+ - \sigma_q^-)/\sigma$ , where  $q = u$  or  $d$ ,  $\sigma^{+(-)}$  is the forward (backward) cross section, and  $\sigma$  is the total cross section from quarks of all charges. Thus, the overall asymmetry is the sum of the asymmetries identified by the  $u$  or  $d$  labels.

partons. Consequently, the asymmetry distribution is sensitive to both  $\sin^2 \theta_W$  and the parton distribution functions (PDF) of the proton.

## II. MEASUREMENTS

In this section, the CDF and D0 measurements used in the combination are briefly summarized. Both measurements are legacy measurements that use the full Tevatron Run II data samples.

### A. D0 summary

The D0 measurement consists of the published electron-channel determination of  $\sin^2 \theta_{\text{eff}}^{\text{lept}}$  [13]. The measurement using muon pairs is not yet available. It is envisioned that the combined

D0 result incorporating the electron and muon channels will be used in the future as input to the final CDF and D0  $A_{fb}$  combination.

The asymmetry  $A_{fb}$  is measured using events with at least two electromagnetic (EM) clusters reconstructed in the calorimeter. They are required to be in the central calorimeter (CC) or end calorimeter (EC) with transverse momentum  $p_T > 25$  GeV/c, and to have shower shapes consistent with that of an electron. Spatially matched tracks reconstructed in the tracking system with  $p_T > 10$  GeV/c and satisfying track quality criteria are further required. Compared to previous D0 results [11, 12], the geometric acceptance in detector pseudorapidity ( $\eta_{det}$ ) is extended from  $|\eta_{det}| < 1.0$  to  $|\eta_{det}| < 1.1$  for CC and from  $1.5 < |\eta_{det}| < 2.5$  to  $1.5 < |\eta_{det}| < 3.2$  for EC. Also, previously rejected electrons reconstructed near azimuthal CC module boundaries are included. By extending the  $\eta_{det}$  and module boundary acceptance, a 70% increase is achieved in the number of events above what would be expected from luminosity increase. Events are categorized as CC-CC, CC-EC or EC-EC based on the  $\eta_{det}$  regions of the two EM candidates.

An improved method of electron energy calibration is developed and applied to both data and MC. In addition to the scale factors used in the previous energy calibration, offset parameters are applied to the electron energy. All parameters are functions of  $\eta_{det}$  and instantaneous luminosity. With this method, the systematic uncertainty due to energy modeling is reduced to a negligible level.

The backgrounds are from the production of QCD dijets,  $W + \text{jets}$ ,  $\gamma^*/Z \rightarrow \tau\tau$ , diboson ( $WW$  and  $WZ$ ), and  $t\bar{t}$ . QCD dijet backgrounds are estimated using the data. The other backgrounds are estimated with PYTHIA 6.23 [23]. At the  $Z$ -boson peak, the overall background level is 0.35%.

The  $A_{fb}$  templates are calculated with the PYTHIA 6.23 LO Drell-Yan generator and the NNPDF 2.3 (NLO) [24] PDFs, and are reweighted to incorporate higher-order QCD effects. The boson distribution as a function of rapidity and transverse momentum ( $y, p_T$ ) is reweighted in both variables to match that from RESBOS [25–28] with CTEQ6.6 [29] PDFs. The boson-mass distribution is reweighted with an NNLO K-factor [30, 31]. The events are processed by the D0 detector simulation to yield templates that include detector resolution effects. The sensitivity of  $A_{fb}$  to QED final-state radiation (FSR) effects is significantly reduced by the inclusion of FSR photons (in an  $\eta/\phi$  cone of  $0.2 \times 0.2$ ) in the electron energy reconstruction.

The raw  $A_{fb}$  distributions in data are obtained for CC-CC, CC-EC and EC-EC event categories as a function of mass. Since the solenoid and toroid polarities are reversed every two weeks on average at D0, the raw distributions of the samples corresponding to the four different solenoid and toroid polarity combinations are weighted by integrated luminosities and summed over the four categories. This weighted combination provides cancellation of asymmetries due to variations in detector response and acceptance with  $\eta_{det}$  and  $p_T$ . The weak mixing angle is extracted from the background-subtracted  $A_{fb}$  spectrum in the regions  $75 < M_{ee} < 115 \text{ GeV}/c^2$  for CC-CC and CC-EC events, and  $81 < M_{ee} < 97 \text{ GeV}/c^2$  for EC-EC events by comparing the data to simulated  $A_{fb}$  templates corresponding to different input values of  $\sin^2 \theta_W$ .

Combining the weak mixing angle results from the three event categories gives

$$\begin{aligned} \sin^2 \theta_{\text{eff}}^{\text{lept}} &= 0.23139 \pm 0.00043 \text{ (stat.)} \\ &\pm 0.00008 \text{ (syst.)} \\ &\pm 0.00017 \text{ (PDF)}. \end{aligned} \tag{8}$$

The systematic uncertainties are shown in Table I [13], and include the sources: energy calibration, energy smearing, backgrounds, charge misidentification, and electron misidentification. The largest component is the electron misidentification (0.00007) and the contribution from background is 0.00001. The PDF uncertainty is obtained using 100 equally probable ensemble PDFs of NNPDF 2.3.

The  $A_{fb}$  templates based on PYTHIA use the same fixed value of the effective coupling  $\sin^2 \theta_{\text{eff}}$  for the lepton,  $u$ -quark, and  $d$ -quark vertices. However, these differ in the corrections between ZFITTER [20–22], used in the CDF measurement, and ZGRAD [32], used by D0. These calculations give complex valued corrections to the Born level couplings and  $\sin^2 \theta_W$ . Relative to  $\sin^2 \theta_{\text{eff}}^{\text{lept}}$ , the value of the real part of  $\sin^2 \theta_{\text{eff}}$  at the  $Z$ -pole mass for the  $u$ - and  $d$ -quarks are shifted by  $-0.0001$  and  $-0.0002$ , respectively. A version of RESBOS with CTEQ6.6 PDFs has been modified to include these real-valued shifts to the  $u$ - and  $d$ -quark  $\sin^2 \theta_{\text{eff}}$  couplings, thus improving the accuracy of the extracted value of  $\sin^2 \theta_{\text{eff}}^{\text{lept}}$ . The  $\sin^2 \theta_{\text{eff}}^{\text{lept}}$  value in PYTHIA is shifted by  $-0.00008$ , with no change in uncertainties. Applying this correction to the measured value gives the final measurement value of  $\sin^2 \theta_{\text{eff}}^{\text{lept}} = 0.23147 \pm 0.00047$ . Both RESBOS and PYTHIA include the same correction for the “running” of the electromagnetic coupling  $\alpha_{\text{em}}$  with the mass scale.



## B. CDF summary

The CDF measurement combines results from the muon [9] and electron [10] channels. Similar methods are used for both analyses. The  $A_{\text{fb}}$  measurements are corrected for detector effects. The effects of detector resolution and QED FSR are removed from the measurements using the simulation. The templates are strictly QCD calculations of  $A_{\text{fb}}$ .

The  $A_{\text{fb}}$  measurement uses the data-driven event-weighting method [33], which is equivalent to individual measurements of  $A_{\text{fb}}$  in  $|\cos\vartheta|$  bins that are then combined. With event weighting, the two separate steps are merged into a single asymmetry measurement using weighted events. The asymmetry in a  $|\cos\vartheta|$  bin is evaluated using

$$A_{\text{fb}} = \frac{N^+ / (\epsilon A)^+ - N^- / (\epsilon A)^-}{N^+ / (\epsilon A)^+ + N^- / (\epsilon A)^-}, \quad (9)$$

where  $N^{+(-)}$  and  $(\epsilon A)^{+(-)}$  are the event count, and the combined efficiency ( $\epsilon$ ) and acceptance ( $A$ ) product, respectively, of forward (backward) lepton pairs. An interchange of the charge labels of a lepton pair does not change the detector cells traversed by the lepton pair or the momentum of the lepton in a detector cell, but reverses the sign of the  $\cos\vartheta$  value. As the detector is expected to be charge symmetric for high  $p_{\text{T}}$  leptons, the acceptance and efficiency dependence of the  $A_{\text{fb}}$  measurement cancels out to first order so that

$$A_{\text{fb}} = \frac{N^+ - N^-}{N^+ + N^-}. \quad (10)$$

Small secondary dependencies are removed with the simulation. The value of  $A_{\text{fb}}$  is proportional to  $A_4$  times angular factors from the event difference of the numerator and event sum of the denominator. These factors are from the general structure of the angular distribution given in Eq. (5). Event weights for events in the numerator and denominator remove the angular dependencies of the event difference and sum, respectively, and, provide the appropriate statistical weight for the combination of events across  $|\cos\vartheta|$  regions.

Because the event-weighting method needs events for corrections, both measurements and template calculations are restricted to regions with sufficiently large acceptance. The muon-pair rapidity is restricted to  $|y| < 1$ , and the electron-pair rapidity is restricted to  $|y| < 1.7$ . For the electron-channel measurement, one electron must be in the central detector region ( $0.05 < |\eta_{\text{det}}| < 1.05$ ) where there is good tracking with small charge misidentification probability. The

partner electron can be either in the central or forward ( $1.2 < |\eta_{\text{det}}| < 2.8$ ) region. For the muon-channel measurement, both muons must be in the central region,  $|\eta_{\text{det}}| < 1$ .

The simulation of Drell-Yan events uses PYTHIA 6.2 [23] with CTEQ5L [34] PDFs to generate events. These events are processed by the event simulation, and then followed by the detector simulation based on GEANT-3 and GFLASH [35]. The event simulation includes PHOTOS 2.0 [36–38], which adds QED FSR from decay particles. For the muon-channel measurement, the generator-level  $p_T$  distribution of the boson is adjusted so that the shape of the reconstruction-level, simulated  $p_T$  distribution matches the data. For the electron-channel measurement, the PYTHIA+PHOTOS calculation is adjusted using the data and the RESBOS calculation. The generator-level  $p_T$  distribution of the boson is adjusted so that the shape of the reconstruction-level simulated  $p_T$  distribution matches the data in two rapidity bins:  $0 < |y| < 0.8$  and  $|y| \geq 0.8$ . The generator-level boson-mass distribution is adjusted with a mass-dependent factor, which is the ratio of the RESBOS boson-mass distribution calculated using CTEQ6.6 PDFs relative to the PYTHIA 6.4 [39] boson-mass distribution calculated using CTEQ5L PDFs.

The energy scale of both the data and simulation are calibrated to a common standard using the technique described in Ref. [40]. The energy resolution of the simulation is calibrated to the data. In addition to the generator level tuning, other distributions such as the time dependent Tevatron beam luminosity profile, and detector responses near boundaries are tuned. Response adjustments are always with symmetric variables such as  $|\eta_{\text{det}}|$  or  $|\cos\vartheta|$ . They are needed for an accurate detector resolution unfolding of the asymmetry distribution in mass and  $\cos\vartheta$  for the data. The unfolding removes the effects of resolution smearing and QED FSR. The simulation is also used to derive the error matrix for the  $A_{\text{fb}}$  measurement.

The backgrounds are from the production of QCD dijets,  $W + \text{jets}$ ,  $\gamma^*/Z \rightarrow \tau\tau$ , diboson ( $WW$ ,  $WZ$ , and  $ZZ$ ), and  $t\bar{t}$ . QCD dijet backgrounds are estimated using the data. Other backgrounds are estimated with PYTHIA 6.2 [23]. For the muon-channel, the overall background level amounts to 0.5%. For the electron channel, the overall background level amounts to about 1.1%. All backgrounds are subtracted from the data.

The  $A_{\text{fb}}$  templates for the electron channel are calculated using the POWHEG-BOX NLO implementation [41] of the Drell-Yan process [42] followed by PYTHIA 6.41 [39] parton-showering. The combined implementation has next-to-leading log resummation accuracy. The NNPDF-3.0 [24, 43–49] NNLO PDFs are used for the parton fluxes. The NNPDF 3.0 parton distributions

consist of an ensemble of 100 equally probable PDFs, and the Giele-Keller (GK) method [50–52] is used to derive the value of an observable and its PDF uncertainty for the ensemble. The complex valued ZFITTER form factors are incorporated into the POWHEG-BOX amplitudes as specified in the Appendix. The QED photon propagator correction from fermion loops is also included; the effect of the real part of this form factor is known as the running  $\alpha_{\text{em}}$ . The implementation of these form factors provides an enhanced Born approximation (EBA) to the electroweak couplings. For consistency with the ZFITTER calculations, the NNPDFs selected are derived with a value of the strong-interaction coupling of 0.118 at the  $Z$  mass. With ZFITTER corrections, the electroweak mixing parameter for the templates is the static on-shell  $\sin^2 \theta_W$ . The asymmetry is directly sensitive to effective couplings, which are provided by ZFITTER. The effective couplings have the form  $\kappa_f \sin^2 \theta_W$ , where  $\kappa_f$  denotes a fermion-flavor ( $f$ ) dependent form factor. Unlike the directly observable effective coupling,  $\sin^2 \theta_W$  and  $\kappa_f$  are inferred in the context of the standard model and its inputs specified in the Appendix. For comparisons with other measurements, the value of the effective leptonic coupling  $\sin^2 \theta_{\text{eff}}^{\text{lept}}$  is defined at the  $Z$  pole and its value is  $\text{Re}[\kappa_e(m_Z^2)] \sin^2 \theta_W$ .

The electron-channel-only result (from Table V of Ref. [10]) is

$$\begin{aligned} \sin^2 \theta_{\text{eff}}^{\text{lept}} &= 0.23248 \pm 0.00049 \quad (\text{stat.}) \\ &\pm 0.00004 \quad (\text{syst.}) \\ &\pm 0.00019 \quad (\text{PDF}). \end{aligned} \tag{11}$$

The systematic uncertainty consists of uncertainties from the energy scale and resolution, the backgrounds, and the QCD scale.

The muon-channel result is

$$\begin{aligned} \sin^2 \theta_{\text{eff}}^{\text{lept}} &= 0.2315 \pm 0.0009 \quad (\text{stat.}) \\ &\pm 0.0002 \quad (\text{syst.}) \\ &\pm 0.0004 \quad (\text{PDF}). \end{aligned} \tag{12}$$

The  $A_{\text{fb}}$  templates are calculated with a modified version of RESBOS using CTEQ6.6 PDFs and the ZFITTER form factors. Systematic uncertainties are estimated using POWHEG-BOX NLO parton generator with CT10 NLO PDFs [53], and followed by PYTHIA 6.41 parton showering. In the publication [9], the PDF uncertainty is derived from the CT10 uncertainty PDFs at

68% C.L.. For the combined result, the muon-channel  $A_{\text{fb}}$  measurement is unchanged but the  $A_{\text{fb}}$  templates are calculated with the same POWHEG-BOX framework with NNPDF 3.0 NNLO PDFs used to calculate the electron-channel templates. The corresponding muon-channel result with templates calculated using POWHEG-BOX with NNPDF 3.0 PDFs is  $\sin^2 \theta_{\text{eff}}^{\text{lept}} = 0.23141 \pm 0.00086$ , where the uncertainty is statistical only.

The CDF result combining electron and muon channels (from Table VI of Ref. [10]) is

$$\begin{aligned} \sin^2 \theta_{\text{eff}}^{\text{lept}} &= 0.23221 \pm 0.00043 \quad (\text{stat.}) \\ &\pm 0.00007 \quad (\text{syst.}) \\ &\pm 0.00016 \quad (\text{PDF}). \end{aligned} \tag{13}$$

The systematic uncertainty consists of uncertainties from the energy scale and resolution, the backgrounds, and the QCD scale (higher order terms).

### III. CORRECTIONS

The CDF and D0 implementations of  $\sin^2 \theta_{\text{eff}}^{\text{lept}}$  differ with regard to the  $A_{\text{fb}}$  templates. The implementations use slightly different methods for weak radiative corrections and different PDFs. In this section, corrections to account for these differences are presented.

#### A. Weak radiative corrections

The  $A_{\text{fb}}$  templates used by D0 are calculated with PYTHIA which uses the same fixed value for the effective couplings  $\sin^2 \theta_{\text{eff}}$  for all fermions. There is only one real-valued weak-mixing angle parameter,  $\sin^2 \theta_{\text{eff}}^{\text{lept}}$ . The value of  $\sin^2 \theta_{\text{eff}}^{\text{lept}}$  extracted from the measured asymmetry distributions is an average over the leptonic,  $u$ -quark, and  $d$ -quark effective couplings, whose values are similar, but not the same. A modified version of RESBOS is used to correct and improve the value of  $\sin^2 \theta_{\text{eff}}^{\text{lept}}$  extracted with the PYTHIA templates. The  $u$ - and  $d$ -quark effective couplings used by RESBOS are shifted by small amounts relative to the leptonic effective coupling. The value of  $\sin^2 \theta_{\text{eff}}^{\text{lept}}$  from PYTHIA templates is shifted by +0.00008 to include the effects of the different  $u$ - and  $d$ -quark effective couplings. By default, PYTHIA and RESBOS use the same implementation of the running  $\alpha_{\text{em}}$ .

The  $A_{\text{fb}}$  templates used by CDF incorporate ZFITTER weak corrections and the fermion-loop correction to the photon propagator, both of which are complex valued and mass-scale dependent. This implementation is denoted as EBA (Enhanced Born Approximation). The effect of using a fixed and constant value for all of the effective couplings is investigated by setting the weak form factors to unity so that the weak mixing angle parameter for the templates becomes  $\sin^2 \theta_{\text{eff}}^{\text{lept}}$ . Only the real part of the photon propagator correction, the running  $\alpha_{\text{em}}$ , is retained. This implementation, denoted as nonEBA, is the analog to the PYTHIA calculation. The difference,

$$\Delta_{\text{eff}}^{\text{lept}} = \sin^2 \theta_{\text{eff}}^{\text{lept}}(\text{EBA}) - \sin^2 \theta_{\text{eff}}^{\text{lept}}(\text{nonEBA}) \quad (14)$$

provides a measure of the correction to the value of  $\sin^2 \theta_{\text{eff}}^{\text{lept}}$  derived using PYTHIA templates needed to convert it to the value derived using ZFITTER form factors.

The difference is calculated using the combination of the CDF muon- and electron-channel  $A_{\text{fb}}$  measurements. Both nonEBA and EBA template calculations use NNPDF 3.0 NNLO with  $\alpha_s(M_Z) = 0.118$ . Each template contains about  $10^9$  generated events, and the uncertainty of  $A_{\text{fb}}$  for the mass bin containing the  $Z$ -boson mass is about  $5 \times 10^{-5}$ . Differences are calculated for 23 ensemble PDFs whose extracted value of the mixing angle is near the measurement value derived from all ensemble PDFs. The GK-weighted average and rms of  $\Delta_{\text{eff}}^{\text{lept}}$  over the partial set of PDFs are 0.00022 and 0.00002, respectively. There is a small PDF dependence. To accommodate the statistical uncertainty of the measurement value of the mixing angle, an additional uncertainty of 0.00003 is assigned, resulting in a total uncertainty of  $\pm 0.00004$ .

The correction to convert  $\sin^2 \theta_{\text{eff}}^{\text{lept}}$  values derived from nonEBA templates to equivalent EBA derived values is  $+0.00022 \pm 0.00004$ . This value is the correction from the PYTHIA framework with a single value for all the effective mixing angles to the ZFITTER based one. As discussed in Sec. II A, the D0 value of  $\sin^2 \theta_{\text{eff}}^{\text{lept}}$  includes a correction of  $+0.00008$  that partially corrects for the differences in the effective mixing angles. The adjustment that standardizes the D0 measurement of  $\sin^2 \theta_{\text{eff}}^{\text{lept}}$  to one based on ZFITTER based corrections, denoted by  $\Delta \sin^2 \theta_{\text{eff}}^{\text{lept}}(\text{ZFITTER})$ , is  $\Delta_{\text{eff}}^{\text{lept}} - 0.00008$ , or  $+0.00014 \pm 0.00004$ .

## B. PDF choice

The D0  $A_{\text{fb}}$  template calculations use NNPDF 2.3; CDF calculations use NNPDF 3.0 NNLO with  $\alpha_s(M_Z) = 0.118$ . The  $A_{\text{fb}}$  calculations using NNPDF 2.3 and 3.0 produce different extracted values of  $\sin^2 \theta_{\text{eff}}^{\text{lept}}$ . NNPDF 3.0 [24, 43–49] includes new HERA and LHC data, and replaces the Tevatron  $W$ -asymmetry measurements with lepton-asymmetry measurements from the LHC. In addition, the technical implementation of PDFs is improved in NNPDF 3.0.

For these reasons, NNPDF 3.0 is preferred for the combination. The value of  $\sin^2 \theta_{\text{eff}}^{\text{lept}}$  is extracted using the default PDF of NNPDF 3.0 and multiple NNPDF 2.3 templates. A Pythia template of 500 million events is generated, using NNPDF 3.0 with fixed  $\sin^2 \theta_W$  input, and taken as pseudo-data after applying fast simulation kinematic cuts; 40 templates of 300 million events each are generated, using NNPDF 2.3 with varying  $\sin^2 \theta_W$  inputs and applying the same cuts. These are used to obtain the best  $\chi^2$  fit for the  $\sin^2 \theta_W$  value. The difference between the input value for NNPDF 3.0 and the value extracted from NNPDF 2.3, denoted by  $\Delta \sin^2 \theta_{\text{eff}}^{\text{lept}}(\text{PDF})$ , is used to provide a correction to the value of  $\sin^2 \theta_{\text{eff}}^{\text{lept}}$  derived using NNPDF 2.3 to that derived using NNPDF 3.0.

The value of  $\Delta \sin^2 \theta_{\text{eff}}^{\text{lept}}(\text{PDF})$  based on the D0 analysis is  $-0.00024 \pm 0.00004$ , where the uncertainty is statistical. A similar calculation in the CDF framework confirms this value.

## IV. CDF AND D0 COMBINATION

The combination of  $\sin^2 \theta_{\text{eff}}^{\text{lept}}$  discussed in this section is based on the D0 electron-channel results [13], and the CDF combined muon- and electron-channel results [10].

### A. Application of corrections to the D0 $A_{\text{fb}}$

The published central value of the D0  $\sin^2 \theta_{\text{eff}}^{\text{lept}}$  measurement is 0.23147. To update this measurement to one based on templates calculated with NNPDF 3.0 PDFs and ZFITTER-based electroweak radiative corrections, two additive adjustments are applied to the central value: a)  $\Delta \sin^2 \theta_{\text{eff}}^{\text{lept}}(\text{PDF}) = -0.00024 \pm 0.00004$ , and b)  $\Delta \sin^2 \theta_{\text{eff}}^{\text{lept}}(\text{ZFITTER}) = +0.00014 \pm 0.00004$ ,

Table I: Summary of the total D0 systematic uncertainties on electron-channel measurement of the electroweak-mixing parameter  $\sin^2 \theta_{\text{eff}}^{\text{lept}}$ .

Source	$\sin^2 \theta_{\text{eff}}^{\text{lept}}$
Energy calibration	$\pm 0.00001$
Energy smearing	$\pm 0.00002$
Background	$\pm 0.00001$
Charge misidentification	$\pm 0.00003$
Electron identification	$\pm 0.00007$
Fiducial asymmetry	$\pm 0.00001$
NNPDF-2.3 PDF	$\pm 0.00017$

Table II: Summary of the CDF systematic uncertainties on the muon- and electron-channel combination for the electroweak-mixing parameter  $\sin^2 \theta_{\text{eff}}^{\text{lept}}$ .

Source	$\sin^2 \theta_{\text{eff}}^{\text{lept}}$
Energy scale and resolution	$\pm 0.00002$
Backgrounds	$\pm 0.00003$
QCD scale	$\pm 0.00006$
NNPDF-3.0 PDF	$\pm 0.00016$

where both uncertainties are statistical. The net correction is  $-0.00010 \pm 0.00005$ , where the uncertainty is denoted as the “correction” uncertainty. The adjusted central value of  $\sin^2 \theta_{\text{eff}}^{\text{lept}}$  is 0.23137, and this value is used when CDF and D0 results are combined.

## B. Combination

The input CDF and D0 measurements are

$$\sin^2 \theta_{\text{eff}}^{\text{lept}}(\text{D0}) = 0.23137 \pm 0.00043, \text{ and} \quad (15)$$

$$\sin^2 \theta_{\text{eff}}^{\text{lept}}(\text{CDF}) = 0.23221 \pm 0.00043, \quad (16)$$

where the uncertainties are statistical only. The systematic uncertainties are summarized in Tables I and II and, except for the PDF uncertainties, are reproduced line-by-line from the

Table III: Summary of the combined uncertainties for the CDF and D0 measurements of the electroweak-mixing parameter  $\sin^2 \theta_{\text{eff}}^{\text{lept}}$ .

Source	Uncertainties on $\sin^2 \theta_{\text{eff}}^{\text{lept}}$		
	CDF Inputs	D0 Inputs	CDF and D0 Combination
Statistics	$\pm 0.00043$	$\pm 0.00043$	$\pm 0.00030$
Uncorrelated	$\pm 0.00007$	$\pm 0.00008$	$\pm 0.00005$
Correction		$\pm 0.00005$	$\pm 0.00003$
NNPDF PDF	$\pm 0.00016$	$\pm 0.00017$	$\pm 0.00017$

corresponding tables in Refs. [13] and [10], respectively. D0 avoids a QCD scale uncertainty by incorporating NNLO effects into the  $A_{\text{fb}}$  templates, while CDF avoids sensitivity to lepton identification and detector asymmetry uncertainties through the use of the event-weighting method described in Sec. II B. The PDF uncertainties are treated as 100% correlated. All other systematic uncertainties in Tables I and II are uncorrelated for the CDF and D0 combination. There are some correlations from the common PYTHIA derived backgrounds, but since the overall contribution from the background is small and the detectors are different, the backgrounds are treated as uncorrelated. The  $\pm 0.00005$  correction uncertainty of Sec. IV A, only applies to the D0 measurement. It is uncorrelated from the other uncertainties, and is treated as a separate category of uncertainty for the combination. The total uncorrelated systematic uncertainties for CDF and D0 are  $\pm 0.00007$  and  $\pm 0.00008$ , respectively.

The CDF and D0 measurements are combined using the ‘‘Best Linear Unbiased Estimate’’ (BLUE) method [54]. The method yields a combination value for  $\sin^2 \theta_{\text{eff}}^{\text{lept}}$  is  $0.23179 \pm 0.00030$ , where the uncertainty is the combined statistical uncertainty. The combination weights are approximately equal, and the  $\chi^2$  for the combination is 1.8. Table III summarizes the sources and values of the uncertainty for the combined value of the  $\sin^2 \theta_{\text{eff}}^{\text{lept}}$  mixing parameter. The combination value for  $\sin^2 \theta_{\text{eff}}^{\text{lept}}$  is

$$\sin^2 \theta_{\text{eff}}^{\text{lept}} = 0.23179 \pm 0.00030 \quad (\text{stat.}) \quad (17)$$

$$\pm 0.00006 \quad (\text{syst.}) \quad (18)$$

$$\pm 0.00017 \quad (\text{PDF}), \quad (19)$$

where the second uncertainty is the quadrature combination of the uncorrelated and correction systematic uncertainties. The combined total uncertainty is  $\pm 0.00035$ .



### C. Inference of $\sin^2 \theta_W$

The observed asymmetry is directly sensitive to the effective couplings, and thus  $\sin^2 \theta_{\text{eff}}^{\text{lept}}$  is a direct measurement. In order to obtain  $\sin^2 \theta_W$  and its uncertainty from the measured value of  $\sin^2 \theta_{\text{eff}}^{\text{lept}}$ , and the relationship

$$\sin^2 \theta_{\text{eff}}^{\text{lept}} = \text{Re}[\kappa_e(M_Z^2)] \sin^2 \theta_W, \quad (20)$$

the ZFITTER standard model calculation with a set of input parameters is required. The calculation and parameters specified in the Appendix provide the context for the inference of  $\sin^2 \theta_W$ . The approximate value of the form factor is 1.037. There is a model dependence on the inferred value of  $\sin^2 \theta_W$  due to the uncertainty from the top-quark mass input of the ZFITTER calculation,  $m_t = 173.2 \pm 0.9 \text{ GeV}/c^2$  [55]. The uncertainty from the model dependence is denoted as the ‘‘form factor’’ uncertainty, whose value is  $\pm 0.00008$ .

For the corrected measurement of D0, the preliminary values of  $\sin^2 \theta_{\text{eff}}^{\text{lept}}$ ,  $\sin^2 \theta_W$ , and  $M_W$  are

$$\sin^2 \theta_{\text{eff}}^{\text{lept}} = 0.23137 \pm 0.00043 \pm 0.00019 \quad (21)$$

$$\sin^2 \theta_W = 0.22313 \pm 0.00041 \pm 0.00020 \quad (22)$$

$$M_W = 80.373 \pm 0.021 \pm 0.010 \text{ GeV}/c^2, \quad (23)$$

where the first contribution to the uncertainties is statistical and the second is systematic. All systematic uncertainties are combined in quadrature, including the PDF uncertainty and the correction uncertainty. The sources of systematic uncertainty are specified in Table I. The systematic uncertainty of  $\sin^2 \theta_W$  ( $M_W$ ) includes the form-factor uncertainty.

The preliminary CDF and D0 combination values for  $\sin^2 \theta_{\text{eff}}^{\text{lept}}$ ,  $\sin^2 \theta_W$ , and  $M_W$  are

$$\sin^2 \theta_{\text{eff}}^{\text{lept}} = 0.23179 \pm 0.00030 \pm 0.00017 \quad (24)$$

$$\sin^2 \theta_W = 0.22356 \pm 0.00029 \pm 0.00019 \quad (25)$$

$$M_W = 80.351 \pm 0.015 \pm 0.010 \text{ GeV}/c^2, \quad (26)$$

where the first contribution to the uncertainties is statistical and the second is systematic. All systematic uncertainties are combined in quadrature, and the sources and values of these uncertainties are listed Tables III and IV. The form-factor uncertainty is only included in the

Table IV: Summary of the combined uncertainties for the CDF and D0 inference of the on-shell electroweak-mixing parameter  $\sin^2 \theta_W$ . Except for the statistics source, all other entries are systematic uncertainties.

Source	$\sin^2 \theta_W$
Statistics	$\pm 0.00029$
Uncorrelated	$\pm 0.00005$
Correction	$\pm 0.00003$
NNPDF PDF	$\pm 0.00016$
Form factor ( $m_t = 173.2 \pm 0.9 \text{ GeV}/c^2$ )	$\pm 0.00008$

Table V: LEP-1 and SLD summary of results on  $\sin^2 \theta_{\text{eff}}^{\text{lept}}$  based on these asymmetry measurements at the  $Z$  pole [4]. The  $Q_{\text{FB}}^{\text{had}}$  measurement is based on the hadronic-charge asymmetry from all-hadronic final states.

Measurement	$\sin^2 \theta_{\text{eff}}^{\text{lept}}$
$A_{\text{FB}}^{0,\ell}$	$0.23099 \pm 0.00053$
$\mathcal{A}_\ell(P_\tau)$	$0.23159 \pm 0.00041$
$\mathcal{A}_\ell(\text{SLD})$	$0.23098 \pm 0.00026$
$A_{\text{FB}}^{0,\text{b}}$	$0.23221 \pm 0.00029$
$A_{\text{FB}}^{0,\text{c}}$	$0.23220 \pm 0.00081$
$Q_{\text{FB}}^{\text{had}}$	$0.2324 \pm 0.0012$

systematic uncertainty of  $\sin^2 \theta_W$  and  $M_W$ .

The measurements of  $\sin^2 \theta_{\text{eff}}^{\text{lept}}$  are compared with previous results from the Tevatron, LHC, LEP-1, and SLD in Fig. 3. The hadron collider results are based on  $A_{\text{fb}}$  measurements. The LEP-1 and SLD results on  $\sin^2 \theta_{\text{eff}}^{\text{lept}}$  are from individual asymmetry measurements shown in Table V.

The  $W$ -boson mass inference is compared in Fig. 4 with previous direct and indirect measurements from the Tevatron, NuTeV, LEP-1, SLD, and LEP-2. The direct measurement is from the Tevatron and LEP-2 [56]. The indirect measurements from the Tevatron are derived from the CDF and D0 measurements of  $A_{\text{fb}}$  described in this note, using the same EBA-based method

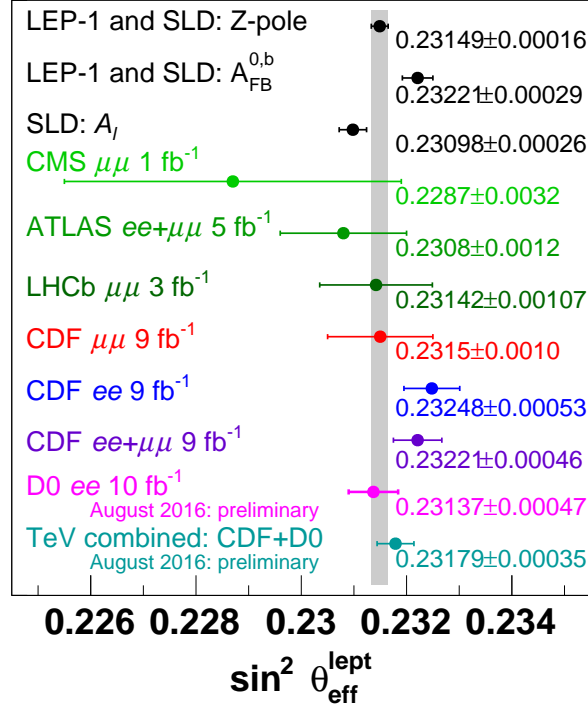


Figure 3: Comparison of experimental measurements of  $\sin^2 \theta_{\text{eff}}^{\text{lept}}$ . The horizontal bars represent total uncertainties. The updated D0 electron-channel result is denoted as “D0  $ee$  10 fb<sup>-1</sup>”. This result is termed preliminary since, although the D0  $A_{FB}$  results are published, the corrections to  $\sin^2 \theta_{\text{eff}}^{\text{lept}}$  discussed in Sec. III are preliminary.

The Tevatron combination of CDF and D0 results is denoted as “TeV combined: CDF+D0”. The other measurements are LEP-1 and SLD [4], CMS [15], ATLAS [14], LHCb [16], and CDF [9, 10]. The LEP-1 and SLD  $Z$  pole result is the combination of their six measurements.

of inference. The indirect measurement of  $\sin^2 \theta_W$  from LEP-1 and SLD,  $0.22332 \pm 0.00039$ , is from the standard model fit to all  $Z$ -pole measurements [4, 5] described in Appendix F of Ref. [5]. The following input parameters to ZFITTER, the Higgs-boson mass  $m_H$ , the  $Z$ -boson mass  $M_Z$ , the QCD coupling at the  $Z$  pole  $\alpha_s(M_Z^2)$ , and the QED correction  $\Delta\alpha_{\text{em}}^{(5)}(M_Z^2)$ , are varied simultaneously within the constraints of the LEP-1 and SLD data, while the top-quark mass  $m_t$  is constrained to the directly measured value from the Tevatron,  $173.2 \pm 0.9$  GeV/ $c^2$  [55]. The NuTeV value is an inference based on the on-shell  $\sin^2 \theta_W$  parameter extracted from the measurement of the ratios of the neutral-to-charged current  $\nu$  and  $\bar{\nu}$  cross sections at Fermilab [57, 58].

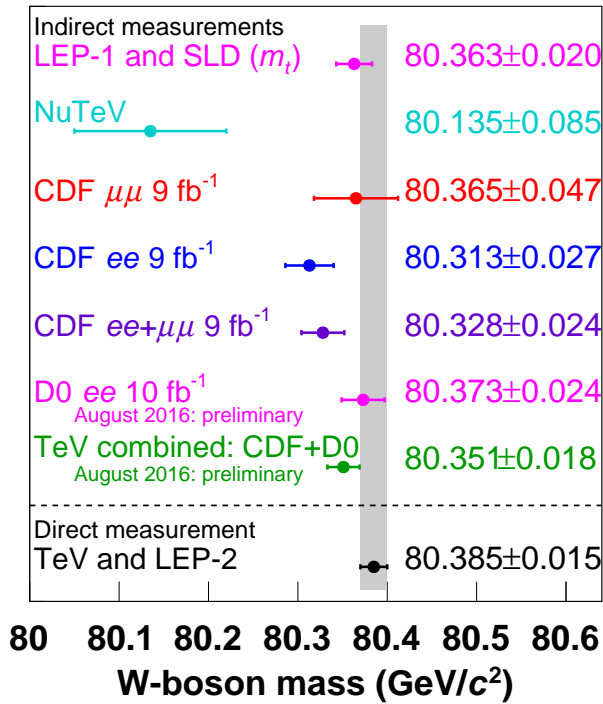


Figure 4: Comparison of experimental determinations of the  $W$ -boson mass. The horizontal bars represent total uncertainties. The updated D0 electron-channel result is denoted as “D0  $ee$  10 fb<sup>-1</sup>”. This result is termed preliminary since, although the D0 Afb results are published, the corrections to  $\sin^2 \theta_{\text{eff}}^{\text{lept}}$  discussed in Sec. III are preliminary.

The Tevatron combination based on CDF and D0 results is denoted as “TeV combined: CDF+D0”. The other indirect measurements are from LEP-1 and SLD [4, 5], which include the Tevatron top-quark mass measurement [55], NuTeV [57, 58], and CDF [9, 10]. The direct measurement is from the Tevatron and LEP-2 [56].

## V. SUMMARY

The angular distribution of Drell-Yan lepton pairs provides information on the electroweak-mixing parameter  $\sin^2 \theta_W$ . The lepton forward-backward asymmetry in the polar-angle distribution  $\cos \vartheta$  is governed by the  $A_4 \cos \vartheta$  term of the helicity cross sections, with the  $A_4$  coefficient directly related to the  $\sin^2 \theta_{\text{eff}}^{\text{lept}}$  mixing parameter at the lepton vertex, and indirectly to  $\sin^2 \theta_W$ . The effective-leptonic parameter  $\sin^2 \theta_{\text{eff}}^{\text{lept}}$  is derived from measurements of the forward-backward asymmetry  $A_{\text{fb}}(M)$  by CDF and D0 based on the full Tevatron datasets. The D0 measurement is derived from electrons pairs from 10 fb<sup>-1</sup> of  $p\bar{p}$  collisions, and the CDF

measurement is derived from both muon and electron pairs from  $9 \text{ fb}^{-1}$  of  $p\bar{p}$  collisions.

The D0 measurement of  $\sin^2 \theta_{\text{eff}}^{\text{lept}}$  has been corrected to include the effects of standard model radiative corrections from ZFITTER, and the updated NNPDF 3.0 parton distribution functions that are employed in the CDF measurement. The updated D0 results are

$$\sin^2 \theta_{\text{eff}}^{\text{lept}} = 0.23137 \pm 0.00047, \quad (27)$$

$$\sin^2 \theta_W = 0.22313 \pm 0.00046, \text{ and} \quad (28)$$

$$M_W(\text{indirect}) = 80.373 \pm 0.024 \text{ GeV}/c^2. \quad (29)$$

Each uncertainty includes statistical and systematic contributions. The inferred value of  $\sin^2 \theta_W$  ( $M_W$ ) is based on the standard model calculations specified in the Appendix. The combination of CDF and D0 results yield

$$\sin^2 \theta_{\text{eff}}^{\text{lept}} = 0.23179 \pm 0.00035, \quad (30)$$

$$\sin^2 \theta_W = 0.22356 \pm 0.00035, \text{ and} \quad (31)$$

$$M_W(\text{indirect}) = 80.351 \pm 0.018 \text{ GeV}/c^2. \quad (32)$$

Both results are consistent with LEP-1 and SLD measurements at the  $Z$ -boson pole.

## VI. ACKNOWLEDGMENTS

We thank the Fermilab staff and the technical staffs of the participating institutions for their vital contributions. This work was supported by DOE and NSF (USA), CONICET and UBACyT (Argentina), ARC (Australia), CNPq and FAPERJ (Brazil), NSERC (Canada), CAS and CNSF (China), Colciencias (Colombia), MSMT (Czech Republic), Marie Curie Fellowship Contract No. 302103 (EU community), Academy of Finland (Finland), CEA and CNRS/IN2P3 (France), BMBF and DFG (Germany), DAE and DST (India), SFI (Ireland), INFN (Italy), Ministry of Education, Culture, Sports, Science and Technology (Japan), World Class University Program and NRF (Korea), CONACyT (Mexico), NSC (Republic of China), MON, NRC KI, and RFBR (Russia), Slovak R&D Agency (Slovakia), Ministerio de Ciencia e Innovación, and Programa Consolider-Ingenio 2010 (Spain), The Swedish Research Council (Sweden), Swiss National Science Foundation (Switzerland), FOM (The Netherlands), MESU (Ukraine), STFC and the Royal Society (UK), and the A.P. Sloan Foundation (USA).

## Appendix A: ZFITTER

The effects of virtual electroweak radiative corrections for the Drell-Yan process are obtained from the  $Z$ -amplitude form factors for fermion-pair production according to  $e^+e^- \rightarrow Z \rightarrow f\bar{f}$ . These form factors are calculated by ZFITTER 6.43 [20–22], which is used with LEP-1, SLD, Tevatron, and LHC measurement inputs for precision tests of the standard model [4, 5].

The input parameters to the ZFITTER radiative-correction calculation are particle masses, the electromagnetic fine-structure constant  $\alpha_{\text{em}}$ , the Fermi constant  $G_F$ , the strong-interaction coupling at the  $Z$  mass  $\alpha_s(M_Z^2)$ , and the contribution of the light quarks to the “running”  $\alpha_{\text{em}}$  at the  $Z$  mass  $\Delta\alpha_{\text{em}}^{(5)}(M_Z^2)$ . The scale-dependent couplings are  $\alpha_s(M_Z^2) = 0.118 \pm 0.001$  [59] and  $\Delta\alpha_{\text{em}}^{(5)}(M_Z^2) = 0.0275 \pm 0.0001$  [60]. The mass parameters are  $M_Z = 91.1875 \pm 0.0021$  GeV/ $c^2$  [4, 5],  $m_t = 173.2 \pm 0.9$  GeV/ $c^2$  (top quark) [55], and  $m_H = 125$  GeV/ $c^2$  (Higgs boson). Form factors and the  $Z$ -boson total decay-width  $\Gamma_Z$  are calculated. The central values of the parameters provide the context of the ZFITTER standard model calculations.

ZFITTER uses the on-shell renormalization scheme [3], where particle masses are on-shell and

$$\sin^2 \theta_W = 1 - M_W^2/M_Z^2 \tag{A1}$$

holds to all orders of perturbation theory by definition. If both  $G_F$  and  $m_H$  are specified,  $\sin \theta_W$  is not independent, and is related to  $G_F$  and  $m_H$  by standard model constraints from radiative corrections. To vary the  $\sin \theta_W$  ( $M_W$ ) parameter, the value of  $G_F$  is not constrained. The value of the  $M_W$  is varied over 80.0–80.5 GeV/ $c^2$ , and for each value, ZFITTER calculates  $G_F$  and the form factors. Each set of calculations corresponds to a family of physics models with standard model-like couplings where  $\sin^2 \theta_W$  and the  $G_F$  coupling are defined by the  $M_W$  parameter. The Higgs-boson mass constraint  $m_H = 125$  GeV/ $c^2$  keeps the form factors within the vicinity of standard model fit values from LEP-1 and SLD [4, 5].

The form factors are calculated in the massless-fermion approximation. Consequently, they only depend on the fermion weak isospin and charge, and are distinguished via three indices:  $e$  (electron type),  $u$  (up-quark type), and  $d$  (down-quark type). For the  $ee \rightarrow Z \rightarrow q\bar{q}$  process,

the ZFITTER scattering-amplitude ansatz is

$$\begin{aligned}
A_q = & \frac{i}{4} \frac{\sqrt{2}G_F M_Z^2}{\hat{s} - (M_Z^2 - i\hat{s}\Gamma_Z/M_Z)} 4T_3^e T_3^q \rho_{eq} \\
& [\langle \bar{e} | \gamma^\mu (1 + \gamma_5) | e \rangle \langle \bar{q} | \gamma_\mu (1 + \gamma_5) | q \rangle + \\
& -4|Q_e| \kappa_e \sin^2 \theta_W \langle \bar{e} | \gamma^\mu | e \rangle \langle \bar{q} | \gamma_\mu (1 + \gamma_5) | q \rangle + \\
& -4|Q_q| \kappa_q \sin^2 \theta_W \langle \bar{e} | \gamma^\mu (1 + \gamma_5) | e \rangle \langle \bar{q} | \gamma_\mu | q \rangle + \\
& 16|Q_e Q_q| \kappa_{eq} \sin^4 \theta_W \langle \bar{e} | \gamma^\mu | e \rangle \langle \bar{q} | \gamma_\mu | q \rangle], \tag{A2}
\end{aligned}$$

where  $q = u$  or  $d$ , the  $\rho_{eq}$ ,  $\kappa_e$ ,  $\kappa_q$ , and  $\kappa_{eq}$  are complex-valued form factors, the bilinear  $\gamma$  matrix terms are covariantly contracted, and  $\frac{1}{2}(1 + \gamma_5)$  is the left-handed helicity projector in the ZFITTER convention. The form factors are functions of the  $\sin^2 \theta_W$  parameter and the Mandelstam  $\hat{s}$  variable of the  $e^+e^- \rightarrow Z \rightarrow f\bar{f}$  process. The  $\kappa_e$  form factors of the  $A_u$  and  $A_d$  amplitudes are not equivalent; however, at  $\hat{s} = M_Z^2$ , they are numerically equal.

The  $\rho_{eq}$ ,  $\kappa_e$ , and  $\kappa_q$  form factors can be incorporated into QCD calculations as corrections to the Born-level  $g_A^f$  and  $g_V^f$  couplings,

$$\begin{aligned}
g_V^f & \rightarrow \sqrt{\rho_{eq}} (T_3^f - 2Q_f \kappa_f \sin^2 \theta_W) \text{ and} \\
g_A^f & \rightarrow \sqrt{\rho_{eq}} T_3^f, \tag{A3}
\end{aligned}$$

where  $f = e$  or  $q$ . The resulting current-current amplitude is similar to  $A_q$ , but the  $\sin^4 \theta_W$  term contains  $\kappa_e \kappa_q$ . This difference is eliminated by adding the  $\sin^4 \theta_W$  term of  $A_q$  with the replacement of  $\kappa_{eq}$  with  $\kappa_{eq} - \kappa_e \kappa_q$  to the current-current amplitude. Further details are provided in Ref. [7, 8].

The products  $\kappa_f \sin^2 \theta_W$ , called effective-mixing terms, are directly accessible from measurements of the asymmetry in the  $\cos \vartheta$  distribution. However, neither the  $\sin^2 \theta_W$  parameter nor the  $\hat{s}$ -dependent form factors can be inferred from measurements without assuming the standard model. The effective-mixing terms are denoted as  $\sin^2 \theta_{\text{eff}}$  to distinguish them from the on-shell definition of the  $\sin^2 \theta_W$  parameter of Eq. (A1). The Drell-Yan process is most sensitive to the  $\sin^2 \theta_{\text{eff}}$  term of the lepton vertex,  $\kappa_e \sin^2 \theta_W$ . At the  $Z$  pole,  $\kappa_e$  is independent of the quark flavor, and the flavor-independent value of  $\kappa_e \sin^2 \theta_W$  is commonly denoted as  $\sin^2 \theta_{\text{eff}}^{\text{lept}}$ . For comparisons with other measurements, the value of  $\sin^2 \theta_{\text{eff}}^{\text{lept}}$  at the  $Z$  pole is taken to be

$\text{Re}[\kappa_e(M_Z^2)] \sin^2 \theta_W$ .

---

- [1] S. D. Drell and T.-M. Yan, *Massive Lepton Pair Production in Hadron-Hadron Collisions at High-Energies*, Phys. Rev. Lett. **25**, 316 (1970).
- [2] K. A. Olive *et al.* (Particle Data Group), *Review of Particle Physics*, Chin. Phys. C **38**, 090001 (2014), and 2015 update.
- [3] A. Sirlin, *Radiative Corrections in the  $SU(2)$ - $L \times U(1)$  Theory: A Simple Renormalization Framework*, Phys. Rev. D **22**, 971 (1980).
- [4] The ALEPH, DELPHI, L3, OPAL, SLD Collaborations, the LEP Electroweak Working Group, the SLD Electroweak and Heavy Flavour Groups, *Precision electroweak measurements on the Z resonance*, Phys. Rept. **427**, 257 (2006).
- [5] The ALEPH, DELPHI, L3, OPAL Collaborations, the LEP Electroweak Working Group, *Electroweak Measurements in Electron-Positron Collisions at W-Boson-Pair Energies at LEP*, Phys. Rept. **532**, 119 (2013).
- [6] D. Acosta *et al.* (CDF Collaboration), *Measurement of the forward-backward charge asymmetry of electron positron pairs in  $p\bar{p}$  collisions at  $\sqrt{s} = 1.96$  TeV*, Phys. Rev. D **71**, 052002 (2005).
- [7] T. Aaltonen *et al.* (CDF Collaboration), *Indirect measurement of  $\sin^2 \theta_W$  ( $M_W$ ) using  $e^+e^-$  pairs in the Z-boson region with  $p\bar{p}$  collisions at a center-of-momentum energy of 1.96 TeV*, Phys. Rev. D **88**, 072002 (2013).
- [8] T. Aaltonen *et al.* (CDF Collaboration), *Indirect measurement of  $\sin^2 \theta_W$  ( $M_W$ ) using  $e^+e^-$  pairs in the Z-boson region with  $p\bar{p}$  collisions at a center-of-momentum energy of 1.96 TeV*, Phys. Rev. D **88**, 079905(E) (2013).
- [9] T. Aaltonen *et al.* (CDF Collaboration), *Indirect measurement of  $\sin^2 \theta_W$  (or  $M_W$ ) using  $\mu^+\mu^-$  pairs from  $\gamma^*/Z$  bosons produced in  $p\bar{p}$  collisions at a center-of-momentum energy of 1.96 TeV*, Phys. Rev. D **89**, 072005 (2014).
- [10] T. Aaltonen *et al.* (CDF Collaboration), *Measurement of  $\sin^2 \theta_{\text{eff}}^{\text{lept}}$  using  $e^+e^-$  pairs from  $\gamma^*/Z$  bosons produced in  $p\bar{p}$  collisions at a center-of-momentum energy of 1.96 TeV*, Phys. Rev. D **93**, 112016 (2016).
- [11] V. M. Abazov *et al.* (D0 Collaboration), *Measurement of the forward-backward charge asymmetry and extraction of  $\sin^2 \theta_W^{\text{eff}}$  in  $p\bar{p} \rightarrow Z/\gamma^* + X \rightarrow e^+e^- + X$  events produced at  $\sqrt{s} = 1.96$  TeV*,



- Phys. Rev. Lett. **101**, 191801 (2008).
- [12] V. M. Abazov *et al.* (D0 Collaboration), *Measurement of  $\sin^2 \theta_{\text{eff}}^{\ell}$  and  $Z$ -light quark couplings using the forward-backward charge asymmetry in  $p\bar{p} \rightarrow Z/\gamma^* \rightarrow e^+e^-$  events with  $\mathcal{L} = 5.0 \text{ fb}^{-1}$  at  $\sqrt{s} = 1.96 \text{ TeV}$* , Phys. Rev. D **84**, 012007 (2011).
- [13] V. M. Abazov *et al.* (D0 Collaboration), *Measurement of the effective weak mixing angle in  $p\bar{p} \rightarrow Z/\gamma^* \rightarrow e^+e^-$  events*, Phys. Rev. Lett. **115**, 041801 (2015).
- [14] G. Aad *et al.* (ATLAS Collaboration), *Measurement of the forward-backward asymmetry of electron and muon pair-production in  $pp$  collisions at  $\sqrt{s} = 7 \text{ TeV}$  with the ATLAS detector*, J. High Energy Phys. **09**, 049 (2015).
- [15] S. Chatrchyan *et al.* (CMS Collaboration), *Measurement of the weak mixing angle with the Drell-Yan process in proton-proton collisions at the LHC*, Phys. Rev. D **84**, 112002 (2011).
- [16] R. Aaij *et al.* (LHCb Collaboration), *Measurement of the forward-backward asymmetry in  $Z/\gamma^* \rightarrow \mu^+\mu^-$  decays and determination of the effective weak mixing angle*, J. High Energy Phys. **11**, 190 (2015).
- [17] J. C. Collins and D. E. Soper, *Angular Distribution of Dileptons in High-Energy Hadron Collisions*, Phys. Rev. D **16**, 2219 (1977).
- [18] E. Mirkes, *Angular decay distribution of leptons from  $W$  bosons at NLO in hadronic collisions*, Nucl. Phys. **B387**, 3 (1992).
- [19] E. Mirkes and J. Ohnemus,  *$W$  and  $Z$  polarization effects in hadronic collisions*, Phys. Rev. D **50**, 5692 (1994).
- [20] D. Bardin, M. Bilenky, T. Riemann, M. Sachwitz, and H. Vogt, *Dizet: A Program Package for the Calculation of Electroweak One Loop Corrections for the Process  $e^+e^- \rightarrow f^+f^-$  Around the  $Z_0$  Peak*, Comput. Phys. Commun. **59**, 303 (1990).
- [21] D. Bardin, P. Christova, M. Jack, L. Kalinovskaya, A. Olchevski, S. Riemann, and T. Riemann, *ZFITTER v.6.21: A Semianalytical program for fermion pair production in  $e^+e^-$  annihilation*, Comput. Phys. Commun. **133**, 229 (2001).
- [22] A. Arbuzov, M. Awramik, M. Czakon, A. Freitas, M. Grünewald, K. Monig, S. Riemann, and T. Riemann, *ZFITTER: A Semi-analytical program for fermion pair production in  $e^+e^-$  annihilation, from version 6.21 to version 6.42*, Comput. Phys. Commun. **174**, 728 (2006).
- [23] T. Sjöstrand, P. Edén, L. Lönnblad, G. Miu, S. Mrenna, and E. Norrbin, *High-energy physics event generation with PYTHIA 6.1*, Comput. Phys. Commun. **135**, 238 (2001).
- [24] R. D. Ball *et al.* (NNPDF Collaboration), *Parton distributions with LHC data*, Nucl. Phys. **B867**,

244 (2013).

- [25] G. A. Ladinsky and C.-P. Yuan, *The Nonperturbative regime in QCD resummation for gauge boson production at hadron colliders*, Phys. Rev. D **50**, R4239 (1994).
- [26] C. Balàzs and C.-P. Yuan, *Soft gluon effects on lepton pairs at hadron colliders*, Phys. Rev. D **56**, 5558 (1997).
- [27] F. Landry, R. Brock, P. M. Nadolsky, and C.-P. Yuan, *Tevatron Run-1 Z boson data and Collins-Soper-Sterman resummation formalism*, Phys. Rev. D **67**, 073016 (2003).
- [28] A. Konychev and P. Nadolsky, *Universality of the Collins-Soper-Sterman nonperturbative function in gauge boson production*, Phys. Lett. B **633**, 710 (2006).
- [29] P. M. Nadolsky *et al.* (CTEQ Collaboration), *Implications of CTEQ global analysis for collider observables*, Phys. Rev. D **78**, 103004 (2008).
- [30] R. Hamberg and W.L. van Neerven and T. Matsuura, *A complete calculation of the order  $\alpha_s^2$  correction to the Drell-Yan K factor*, Nucl. Phys. **B359**, 343 (1991).
- [31] R. Hamberg and W.L. van Neerven and T. Matsuura, *A complete calculation of the order  $\alpha_s^2$  correction to the Drell-Yan K factor*, Nucl. Phys. **B644**, 430(E) (2002).
- [32] U. Baur, O. Brein, W. Hollik, C. Schappacher, and D. Wackerroth, *Electroweak radiative corrections to neutral current Drell-Yan processes at hadron colliders*, Phys. Rev. D **65**, 033007 (2002).
- [33] A. Bodek, *A simple event weighting technique for optimizing the measurement of the forward-backward asymmetry of Drell-Yan dilepton pairs at hadron colliders*, Eur. Phys. J. C **67**, 321 (2010).
- [34] H. L. Lai *et al.* (CTEQ Collaboration), *Global QCD analysis of parton structure of the nucleon: CTEQ5 parton distributions*, Eur. Phys. J. C **12**, 375 (2000).
- [35] G. Grindhammer, M. Rudowicz, and S. Peters, *The Fast Simulation of Electromagnetic and Hadronic Showers*, Nucl. Instrum. Methods Phys. Res., Sect. A **290**, 469 (1990).
- [36] E. Barberio and Z. Was, *PHOTOS: A Universal Monte Carlo for QED radiative corrections. Version 2.0*, Computer Phys. Comm. **79**, 291 (1994).
- [37] E. Barberio, B. van Eijk, and Z. Was, *PHOTOS: A Universal Monte Carlo for QED radiative corrections in decays*, Computer Phys. Comm. **66**, 115 (1991).
- [38] P. Golonka and Z. Was, *PHOTOS Monte Carlo: A Precision tool for QED corrections in Z and W decays*, Eur. Phys. J. C **45**, 97 (2006).
- [39] T. Sjöstrand, S. Mrenna, and P. Z. Skands, *PYTHIA 6.4 Physics and Manual*, J. High Energy Phys. **05**, 026 (2006).

- [40] A. Bodek, A. van Dyne, J.-Y. Han, W. Sakumoto, and A. Strelnikov, *Extracting Muon Momentum Scale Corrections for Hadron Collider Experiments*, Eur. Phys. J. C **72**, 2194 (2012).
- [41] S. Frixione, P. Nason, and C. Oleari, *Matching NLO QCD computations with Parton Shower simulations: the POWHEG method*, J. High Energy Phys. **11**, 070 (2007).
- [42] S. Alioli, P. Nason, C. Oleari, and E. Re, *NLO vector-boson production matched with shower in POWHEG*, J. High Energy Phys. **07**, 060 (2008).
- [43] R. D. Ball *et al.* (NNPDF Collaboration), *Parton distributions for the LHC Run II*, J. High Energy Phys. **04**, 040 (2015).
- [44] R. D. Ball, V. Bertone, F. Cerutti, L. D. Debbio, S. Forte, A. Guffanti, J. I. Latorre, J. Rojo, and M. Ubiali (NNPDF Collaboration), *Unbiased global determination of parton distributions and their uncertainties at NNLO and at LO*, Nucl. Phys. **B855**, 153 (2012).
- [45] R. D. Ball, V. Bertone, F. Cerutti, L. D. Debbio, S. Forte, A. Guffanti, J. I. Latorre, J. Rojo, and M. Ubiali (NNPDF Collaboration), *Impact of Heavy Quark Masses on Parton Distributions and LHC Phenomenology*, Nucl. Phys. **B849**, 296 (2011).
- [46] R. D. Ball, L. D. Debbio, S. Forte, A. Guffanti, J. I. Latorre, J. Rojo, and M. Ubiali (NNPDF Collaboration), *A first unbiased global NLO determination of parton distributions and their uncertainties*, Nucl. Phys. **B838**, 136 (2010).
- [47] R. D. Ball, L. D. Debbio, S. Forte, A. Guffanti, J. I. Latorre, A. Piccione, J. Rojo, and M. Ubiali (NNPDF Collaboration), *A Determination of parton distributions with faithful uncertainty estimation*, Nucl. Phys. **B809**, 1 (2009).
- [48] R. D. Ball, L. D. Debbio, S. Forte, A. Guffanti, J. I. Latorre, A. Piccione, J. Rojo, and M. Ubiali (NNPDF Collaboration), *A Determination of parton distributions with faithful uncertainty estimation*, Nucl. Phys. **B816**, 293(E) (2009).
- [49] S. Forte, L. Garrido, J. I. Latorre, and A. Piccione, *Neural network parametrization of deep inelastic structure functions*, J. High Energy Phys. **05**, 062 (2002).
- [50] W. T. Giele and S. Keller, *Implications of hadron collider observables on parton distribution function uncertainties*, Phys. Rev. D **58**, 094023 (1998).
- [51] N. Sato, J. F. Owens, and H. Prosper, *Bayesian Reweighting for Global Fits*, Phys. Rev. D **89**, 114020 (2014).
- [52] A. Bodek, J.-Y. Han, A. Khukhunaishvili, and W. Sakumoto, *Using Drell-Yan forward-backward asymmetry to reduce PDF uncertainties in the measurement of electroweak parameters*, Eur. Phys. J. C **76**, 115 (2016).

- [53] H.-L. Lai, M. Guzzi, J. Huston, Z. Li, P. Nadolsky, J. Pumplin, and C.-P. Yuan, *New parton distributions for collider physics*, Phys. Rev. D **82**, 074024 (2010).
- [54] L. Lyons, D. Gibaut, and P. Cliffort, *How to Combine Correlated Estimates of a Single Physical Quantity*, Nucl. Instrum. Methods Phys. Res., Sect. A **270**, 110 (1988).
- [55] T. Aaltonen *et al.* (CDF and D0 Collaborations), *Combination of the top-quark mass measurements from the Tevatron collider*, Phys. Rev. D **86**, 092003 (2012).
- [56] T. Aaltonen *et al.* (CDF and D0 Collaboration), *Combination of CDF and D0 W-Boson Mass Measurements*, Phys. Rev. D **88**, 052018 (2013).
- [57] G. P. Zeller *et al.* (NuTeV Collaboration), *A Precise determination of electroweak parameters in neutrino nucleon scattering*, Phys. Rev. Lett. **88**, 091802 (2002).
- [58] G. P. Zeller *et al.* (NuTeV Collaboration), *A Precise determination of electroweak parameters in neutrino nucleon scattering*, Phys. Rev. Lett. **90**, 239902(E) (2003).
- [59] S. Bethke, *The 2009 World Average of  $\alpha(s)$* , Eur. Phys. J. C **64**, 689 (2009).
- [60] F. Jegerlehner, *Electroweak effective couplings for future precision experiments*, Nuovo Cim. C **034S1**, 31 (2011).